Environ. Sci. Technol. 1984, 18, 860–868

Photoreductive Dissolution of Colloidal Iron Oxides in Natural Waters

T. David Waite* and François M. M. Morel

Ralph M. Parsons Laboratory, Massachusetts Institute of Technology, Cambridge, Massachusetts 02139

■ Size-separation (0.1-μm filtration and ultrafiltration) techniques and coulometric procedures have been used to investigate the photoreductive dissolution of iron oxides under conditions typical of natural waters. In the absence of organic agents, iron oxides are solubilized to varying degrees through photodissociation of ferric hydroxy groups at the colloid surface. The degree of dissolution is dependent principally on the chromophore concentration and is highest at low pH and high colloidal surface area. Naturally occurring organic materials significantly increase the initial rate of dissolution. Despite the enhancement by organic agents significant effects of light on net dissolution are only observed at low pH. Irradiation of natural waters produces hydrogen peroxide in quantities sufficient to markedly affect the solution-phase speciation of iron and under certain conditions (e.g., seawater) also affects the net photodissolution of iron oxides.

Introduction

In recent years increased attention has been given to sunlight-induced photochemical effects in marine and freshwater environments with a number of detailed, systematic studies providing considerable insight into the nature and importance of selected processes (*1–3*). While significant progress has been made, the complexity of the aquatic systems of interest and the resultant difficulty in identifying the primary and secondary photoprocesses involved place severe limitations on the chemical entities amenable to study. Of particular interest but of troublesome complexity are the effects of light on the chemistry of iron in natural waters.

The photoreactivity of both organic and inorganic complexes of iron has long been recognized, and many reports of the effects of light on the chemistry of iron have been published over the last 100 years (*4*). In addition, a number of studies on natural waters have indicated that sunlight may be effective in inducing changes in iron speciation in aquatic systems through reduction of ferric iron species (*5–8*) and/or dissolution of colloidal iron oxides (*8*). All of these natural water studies have been performed in acidic lakes; however, there has also been speculation (*9*) that light may be important in increasing the availability of iron to aquatic organisms in marine systems through dissolution of colloidal iron oxides. In this paper we attempt to clarify the significance of light-induced changes in iron speciation in natural waters through examination of the photodissolution of colloidal iron oxides under conditions typical of marine and freshwater environments.

We have recently reported on the effect of citrate—a strong ferric iron complexing agent—in enhancing the photodissolution of γ-FeOOH (*10*) and have presented a simple scheme detailing the major steps involved in this dissolution process. This scheme, which is shown in Figure 1 for an iron oxyhydroxide ≡FeOOH and a ligand L, principally involves the photodegradation of iron–organic groups at the colloid surface resulting in the reduction of Fe(III) with concomitant release of reduced iron to solution. Initial dissolution rates were observed to be proportional to the concentration of surface-bound ligand, ≡Fe(III)L. At low pH (pH ≃4) the rate was found to be constant, while at higher pH (6.5 and 8.2), decreasing rates of dissolution were observed as time-dependent back-reactions, and changes in reactant photoactivity became important. Interestingly, the photoreduction of soluble and surface-bound ferric citrate complexes exhibit similar first-order rate constant. Given the similarity in response to light of solution phase and oxide-bound ferric citrate complexes and the known photoactivity of soluble iron–fulvic acid groups (*11*), we might expect to see an enhancement in photoinduced dissolution of colloidal iron oxides in the presence of naturally occurring organic materials such as fulvic acids under certain conditions. This possibility is investigated here through studies of iron oxide photodissolution (a) under relatively well-defined conditions at total iron and organic compound concentrations typical of freshwaters and (b) in synthetic and real ocean waters at concentrations more typical of marine systems. The well-defined studies are performed on the synthesized iron oxide, lepidocrocite (γ-FeOOH), in the presence of two freshwater fulvic acids while amorphous iron oxyhydroxide is used in the seawater studies.

As is clear from the γ-FeOOH–citric acid study (*10*), the dissolution process cannot be studied in isolation since additional processes such as complexation and oxidation may play an important role in determining the net dissolution of iron oxide. Given the known impact of hydrogen peroxide on the aqueous chemistry of iron (*12*) and the observed (possibly light-induced) presence of this powerful oxidizing agent in natural waters (*13–15*), particular attention is given here to its existence in the systems under investigation and to its effect on the speciation of iron.

Experimental Section

Procedure for Well-Defined System Studies. The procedure for investigating the photodissolution of γ-FeOOH in the absence and presence of fulvic acids is similar to that used previously in studies of the effect of citrate on the photodissolution of lepidocrocite (*10*) and thus is described only briefly here. All dissolution measurements were performed in a 300-mL water-jacketed glass vessel with quartz windows at both ends and access ports enabling sample extraction. The total amount of iron remaining in suspension and the amount of 0.1-μm Nuclepore filterable iron at various times after addition of 5 μM radiolabeled γ-FeOOH to pH 4.0 and 6.5 solutions of 0.1 M NaCl containing 10 mg/L of fulvic acid were determined under dark and light conditions by using liquid scintillation techniques. Studies were typically conducted for 165 min under dark conditions prior to investigating the effects of light. While some uncertainty exists as to the extent of fulvic acid adsorption to the iron oxide colloid within this time, a majority of the available surface sites are likely to be occupied by organic molecules (cf. the results of studies on citrate adsorption to lepidocrocite indicating ≃80% of adsorption capacity reached after 165 min (*10*)). The pH 4.0 solutions were obtained by addition of hydrochloric acid while the pH 6.5 solutions were prepared by addition of sodium bicarbonate and equilibration with a CO_2/air mixture of proportion necessary to produce the desired pH. All solutions were vigorously stirred and maintained at 20 °C.

0013-936X/84/0918-0860$01.50/0

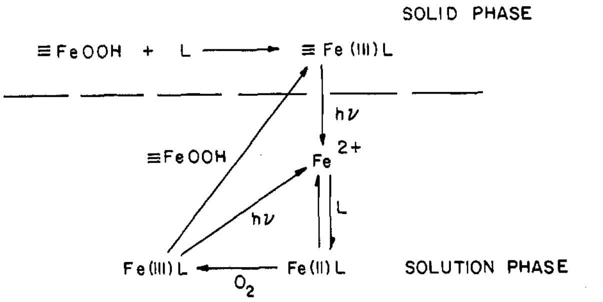

Figure 1. Simple conceptual model of the major processes operating in an irradiated system containing colloidal iron oxide and ligand L.

The concentration of peroxides (H_2O_2 and organic peroxides) produced on irradiation of 10 mg/L solutions of fulvic acid in 0.1 M NaCl at various pH values (with no added iron) was determined by measuring the extent of the peroxidase-catalyzed destruction of highly fluorescent scopoletin (6-methoxy-7-hydroxy-1,2-benzopyrone). Details of the technique are described by Zika et al. (*16*). The oxidation of Fe(II) added to 0.1 M NaCl in the absence and presence of excess H_2O_2 was investigated at pH 4.0 and pH 6.5 by colorimetrically monitoring the concentration of Fe(II) remaining in solution over time. Initial Fe(II) and H_2O_2 concentrations of 3 and 10 μM, respectively, were used.

Procedure for Marine System Studies. These studies were typically conducted in solutions containing $<10^{-7}$ M total added iron and thus required the addition of particularly radioactive colloids in order that the concentration of filterable iron be measurable by liquid scintillation techniques. Because of the difficulty (and expense) of preparing highly radioactive colloids of defined structure (such as lepidocrocite) and the desire to use colloids possessing surface area more typical of that for iron oxides from marine waters, amorphous iron oxyhydroxide colloids were used in all such studies. These colloids were prepared in situ by direct addition of ^{59}Fe from acidified $^{59}FeCl_3$ stock to the system of interest. The small size of these amorphous colloids necessitated the use of filters of pore diameter <0.1 μm; thus, Amicon PM10 ultrafilters, possessing a nominal molecular weight cutoff of 10 000, were used in all cases. Preliminary studies of the effect of light on the solubilization of relatively high concentrations of these amorphous colloids were conducted in pH 4.0 Millipore Q-water and in pH 4.0 and 6.5 0.1 M NaCl. In these studies the concentration of Fe(II) produced on irradiation was monitored colorimetrically. Studies involving synthetic and natural seawaters were performed at pH 8.2 (the air-equilibrated pH) and pH 6.5 (obtained by equilibration with a 2.5% CO_2/air mixture). In addition to PM10 ultrafiltration of aliquots extracted periodically from the reaction vessel, coulometric studies of the sample under dark and light conditions were performed as a means of identifying the nature and concentration of photolysis products. The details of controlled potential and "steady-state scanning" coulometric procedures have been given previously (*17*).

The effects of long-term (8 h) UV irradiation on the photodissolution of amorphous iron oxide added to seawater was investigated by performing photodissolution experiments in natural seawater before and after UV irradiation of the seawater samples. The concentration of peroxides present in the seawater samples before and after UV irradiation was measured by using the peroxidase–scopoletin method, and the effect of UV irradiation on the metal binding capacity of the natural seawater was determined by Cu(II)/Cu(I) amperometric titrimetry (*18*). The effect of added H_2O_2 on the photodissolution of amorphous iron oxyhydroxide added to seawater was also investigated.

Ferrous iron oxidation studies were performed in synthetic and natural seawaters at pH 6.5 and 8.2 by monitoring the concentrations of Fe(II) remaining in solution coulometrically (*17*). An initial Fe(II) concentration of 6 nM was used, and all studies were performed at 20 °C.

Materials. The preparation and characterization of the lepidocrocite (γ-FeOOH) used has been described in detail elsewhere (*10*). The γ-FeOOH was radiolabeled by spiking the Fe(II) stock used to prepare the iron oxide with ^{59}Fe(II) produced by electrolyzing $\simeq 10^{-4}$ M $^{59}FeCl_3$ in 10^{-2} M HCl at 200 mV (relative to an Ag/AgCl reference). Preparation of the amorphous iron oxide used in the marine system studies has been described above. Two aquatic fulvic acids extracted from fresh waters were used in this study. Suwanee River fulvic acid is the standard aquatic fulvic acid of the international Humic Substances Society and was supplied by the U.S. Geological Survey. The characteristics of this material have been reported by Thurman and Malcolm (*19*). Grassy Pond fulvic acid was extracted from the surface waters of an acidic central Massachusetts lake by using the methods outlined by Thurman and Malcolm (*20*). The natural seawater was obtained from a Massachusetts coastal region (Nahant) and was used without further treatment after filtration through a 0.2-μm Nuclepore membrane. The preparative procedure and characteristics of the synthetic ocean water (SOW) mixture used are described in detail by Morel et al. (*21*).

Instrumentation. Light was supplied by a Kratos/Schoeffel SS1000 solar simulator system and provided a reasonably well-collimated uniform beam. Appropriate filtering produced a spectrum similar to that of 90° elevation noonday sun. An intensity of approximately 100 mW/cm^2 was provided by the light source with the amount of radiation entering the vessel as determined by ferric–oxalate actinometry (*22*) being 30 μEinsteins (mL of solution)$^{-1}$ min^{-1}. UV irradiation of the Nahant seawater sample (contained in quartz tubes) was provided by a 1200-W mercury discharge lamp. All electrochemical measurements were performed on an Environmental Science Associates Model 3040 charge transfer analyzer using a graphite working electrode, and scopoletin fluorescence was monitored on a Perkin-Elmer LS-5 fluorescence spectrometer.

Results and Discussion

Lepidocrocite Photodissolution in the Presence of Fulvic Acids. As shown in Figure 2a, irradiation of $\simeq$5 μM γ-FeOOH suspended in organic-free 0.1 M NaCl of pH 4.0 results in dissolution of the oxide at a rate of 0.26 nmol of Fe (μmol of γ-FeOOH)$^{-1}$ (min)$^{-1}$. Addition of freshwater fulvic acids induces an approximately 4-fold increase in dissolution rate with 1.0 nmol of Fe solubilized (μmol of γ-FeOOH)$^{-1}$ (min)$^{-1}$ in the presence of 10 mg/L of both Suwanee River fulvic acid (of average M_r 1200) and Grassy Pond fulvic acid. At pH 6.5, no measurable dissolution of γ-FeOOH occurs in the absence of organic materials while a small degree of dissolution is observed in the presence of the fulvic acids. At this pH, initial dissolution rates of 0.35 and 0.20 nmol of Fe solubilized (μmol of γ-FeOOH)$^{-1}$ (min)$^{-1}$ in the presence of Suwanee River and Grassy Pond fulvic acids, respectively, are observed with a decrease in rate on continued photolysis.

Note that, while the amount of light entering the reaction vessel has been determined, no information is available on the proportion of this energy input that is actually absorbed by the dissolved and suspended components of

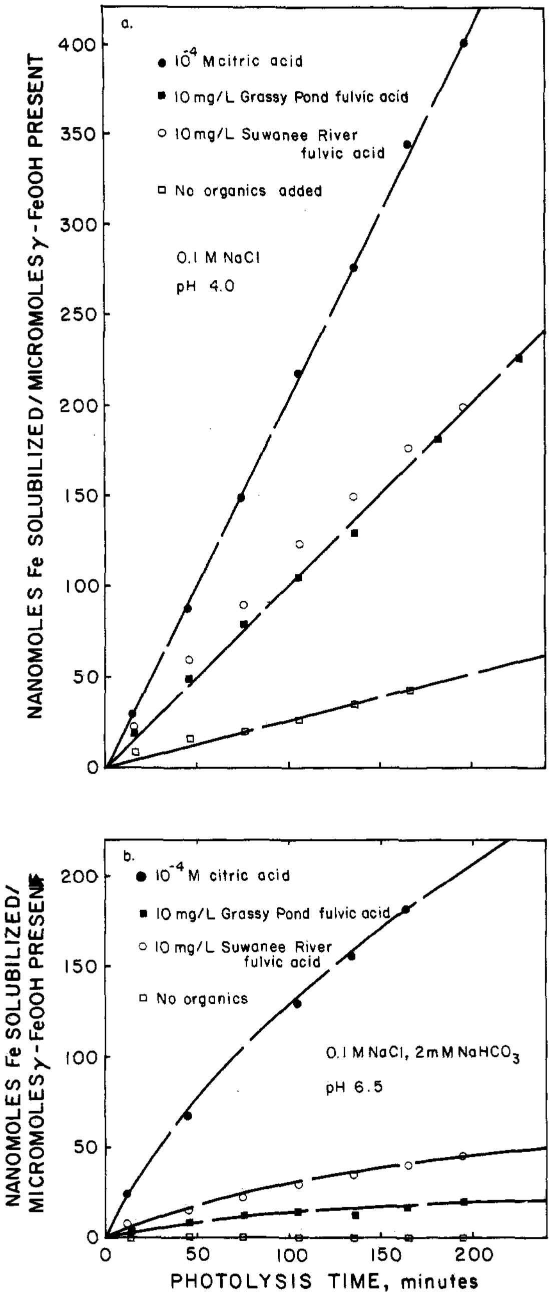

Figure 2. Dissolution (as measured by 0.1-μm filtration) of γ-FeOOH on irradiation of pH 4.0 and pH 6.5 solutions containing either 10^{-4} M citrate, 10 mg/L Suwanee River or Grassy Pond fulvic acids, or no added organic agent. Total radiation input is 30 μEinsteins mL^{-1} min^{-1}.

the system. Qualitatively, it is apparent that a significant portion of the radiation is not absorbed by the constituents of the reaction vessel; however, a more quantitative measure (which would enable estimation of quantum yields) will require detailed wavelength dependency studies.

The results of earlier studies on the citrate-enhanced photodissolution of lepidocrocite performed under similar conditions (*10*) are also included in Figure 2 and indicate that, while citrate enhances γ-FeOOH photodissolution considerably more than do the fulvic acids, the same general effects are observed. In the case of citrate a direct correspondence was found between the concentration of adsorbed citrate (which decreases with increasing pH) and initial photodissolution rate. In addition, the decreasing rate of dissolution at pH 6.5 was attributed to both a decrease in photolability of surface bound groups on continued photolysis and back-reactions resulting in a decrease in concentration of iron species in solution. Similar effects are likely to be operating in an iron oxide–fulvic acid system although additional factors may also be of importance. For example, solution-phase studies of the photodegradation of ferric citrate indicated that this process is relatively pH independent whereas the photodegradation of soluble iron–fulvic acid complexes is very much influenced by pH. Ligand-exchange studies (*11*) of the same fulvic acids as used here indicated that irradiation of iron–fulvic acid mixtures at pH 4.0 results in the rapid formation of reduced iron species while irradiation at pH 6.5 has only a minor effect on the iron–fulvic acid interaction with only small production of Fe(II). Given the apparent similarity between the photolability of surface-bound and solution-phase iron–organic complexes (*10*), the marked decrease in rate of fulvic acid enhanced γ-FeOOH photodissolution observed on increasing the pH from 4.0 to 6.5 is thus to be expected assuming of course that, as in the case of citrate, the photodissolution of γ-FeOOH in the presence of fulvic acids involves the formation of reduced iron species.

The slightly greater initial rate of γ-FeOOH dissolution observed in the presence of Suwanee River fulvic acid compared to Grassy Pond fulvic acid at pH 6.5 is most likely related, at least in part, to the greater ability of Suwanee River fulvic acid to reduce Fe(III). Ligand-exchange studies of the two fulvic acids (*11*) in pH 6.5 solutions containing ≃5 μM total Fe(III) and 10 mg/L fulvic acid showed that Suwanee River fulvic acid will reduce about 20% of the added Fe(III) compared to 14% reduction in the presence of Grassy Pond fulvic acid.

An additional complication in elucidating the mechanism of photoenhanced dissolution of γ-FeOOH in the presence of fulvic acids involves the possibility of direct excitation of the organic molecule by near-UV radiation. In a manner similar to that discussed by Watanabe et al. (*23*) for the rhodamine B–CdS system, the excited fulvic acid molecule may give up an electron to Fe(III) in the iron oxide matrix with resultant reduction and dissolution of the oxide phase. In the absence of data on the relative absorbances of the organic and mineral components of the system, definitive comments concerning the dissolution mechanism cannot be made.

Photoinduced Production and Effects of Hydrogen Peroxide. Another factor which may be of importance in the net dissolution of iron oxides is the possible production of powerful oxidants such as hydrogen peroxide. In the γ-FeOOH–citrate dissolution study (*10*) we showed that superimposed on the dissolution process is a rapid solution-phase redox cycle with the oxidation step controlled by organic complexation and the reduction step induced by light. The relative rates of these redox reactions determines the solution-phase speciation which in turn is the critical factor governing back-reactions in which iron species may be removed from solution (e.g., through "ligand-like" adsorption of Fe(III)L to the oxide). Strong oxidants are likely to perturb this redox cycle with a resultant change in solution-phase speciation. Oxidation of Fe(II) may also be induced at such a rapid rate that hydrolysis of Fe(III) to the insoluble oxide outcompetes organic complexation, resulting in the direct removal of iron from solution.

That irradiation of fulvic acids does produce measurable quantities of hydrogen peroxide (and possibly organic peroxides) is evident from Figure 3 which shows the rate of production of H_2O_2 on irradiation of 10 mg/L Grassy Pond fulvic acid in pH 4 0.1 M NaCl and pH 8.2 0.1 M NaCl–2 mM $NaHCO_3$ for a total radiation input of 30 μEinsteins mL^{-1} min^{-1}. At pH 4.0, approximately 0.6 nM

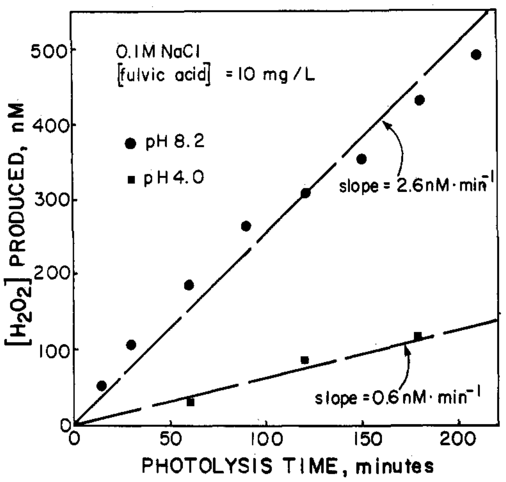

Figure 3. Production of hydrogen peroxide (as measured by the peroxidase-catalyzed destruction of scopoletin fluorescence) on irradiating 10 mg/L solutions of freshwater fulvic acid with simulated solar radiation of total light dosage of 30 μEinsteins mL^{-1} min^{-1}.

H_2O_2 min^{-1} is produced while at pH 8.2 the rate is 4–5 times higher at 2.6 nM min^{-1}. The actual mechanism of production of H_2O_2 is unclear but may involve the superoxide radical anion, O_2^-, which is likely to be present as a result of photoionization of the fulvic acid (*24*):

$$\text{organic chromophore } (S_0) + h\nu \rightarrow S_1 \rightsquigarrow T_1$$

$$\text{Chrom } (S_1 \text{ or } T_1) + O_2 \rightarrow O_2^- + \text{Chrom}^+$$

In aqueous solution O_2^- rapidly disproportionates to H_2O_2 with the equilibrium between O_2^- and H_2O_2 being far to the right (*25*):

$$2O_2^- + 2H^+ \rightleftarrows H_2O_2 + O_2 \qquad K_{\text{pH7}} = 4 \times 10^{20}$$

The involvement of the superoxide radical in the production of H_2O_2 on photolysis of fulvic acids is supported by the recent work of Baxter and Carey (*26*). Alternatively, fulvic acids may act as photosensitizers in the production of singlet oxygen with the formation of H_2O_2 occurring through secondary reactions of $^1O_2$. Such a mechanism could account for the pH dependence of H_2O_2 production seen in Figure 3 since, for some sensitizers, the rate of singlet oxygen production decreases with decrease in pH, the rate of triplet quenching by O_2 being very dependent on the degree of protonation of the sensitizer molecule (*27*).

As can be seen in Figure 4, the presence of excess hydrogen peroxide markedly enhances the rate of Fe(II) oxidation with an immeasurably slow rate of O_2 oxidation at pH 4.0 while the H_2O_2-induced oxidation exhibits a $\tau_{1/2} \simeq 20$ min. At pH 6.5 the $\tau_{1/2}$ values for the O_2- and H_2O_2-induced oxidations under these conditions are observed to be $\simeq$ 3 h and 12 s, respectively. This oxidation constitutes the well-known "Fenton's reagent" reaction (*12*):

$$H_2O_2 + Fe^{2+} \xrightarrow{k_1} Fe^{3+} + HO^- + HO\cdot \qquad k_1 = 76 \text{ L (mol·s)}^{-1}$$

$$HO\cdot + Fe^{2+} \xrightarrow{k_2} Fe^{3+} + HO^- \quad k_2 = 3 \times 10^8 \text{ L (mol·s)}^{-1}$$

Comparison of Figures 2 and 3 indicates that the quantity of H_2O_2 produced is certainly sufficient to influence the rate of oxidation of Fe(II). Thus, on irradiation of a pH 4.0 solution of 10 mg/L Grassy Pond fulvic acid for 1 min we would expect to produce 0.6 nM H_2O_2 and, at most, 1.0 nM Fe(II). As shown above, the rate of H_2O_2-induced oxidation of Fe(II) at this pH is not particularly fast ($\tau_{1/2} \simeq 20$ min); thus, it is likely that any produced Fe(III) will be complexed by the fulvic acid. At pH 6.5, we would expect to produce 1.5 nM H_2O_2 and 0.16 nM Fe(II) on irradiation of the iron–fulvic acid mixture for 1 min; i.e., a large excess of H_2O_2 over Fe(II) is produced. Given the very rapid rate of peroxide-induced oxidation at this pH, it is very likely that hydrolysis of the produced Fe(III) leading to solid oxide formation will compete effectively with organic complex formation. Thus, at pH 4.0, the production of H_2O_2 may well alter the solution speciation of iron but is unlikely to affect net γ-FeOOH dissolution significantly, while at pH 6.5, we may expect a small decrease in net γ-FeOOH photodissolution due to peroxide production and resultant solid ferric oxide formation. The magnitude of this effect will be dependent particularly on the photoreducibility of Fe(III) bound to the fulvic acid at this pH and on the relative rates of Fe(III) complexation by the fulvic acid and Fe(III) hydrolysis.

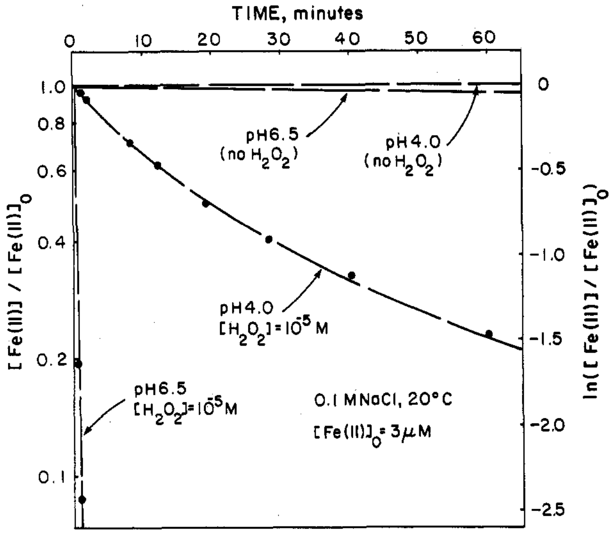

Figure 4. Effect of excess hydrogen peroxide in enhancing rate of oxidation of Fe^{2+} in 0.1 M NaCl at pH 4.0 and 0.1 M NaCl–2 mM $NaHCO_3$ at pH 6.5.

Photodissolution of Amorphous Iron Oxide in Organic-Free Medium. As noted earlier, the net photoinduced dissolution of γ-FeOOH in the absence of added organic agents is small, with no effect observed at pH 6.5 and a rate of only 0.26 nmol of Fe solubilized (μmol of γ-FeOOH)$^{-1}$ min^{-1} at pH 4.0. However, as shown in Figure 5, the effects of light on the dissolution of amorphous colloidal iron oxides and the concomitant production of soluble ferrous iron are much more dramatic. Addition of 3.5 μM Fe(III) to a dark solution of pH 4.0 Q-H_2O results in the formation of nonultrafilterable (presumably colloidal) species which are almost completely solubilized and reduced to Fe(II) after irradiation for 1 h. The initial rate of reduction is particularly rapid with approximately 80 nmol of Fe reduced (μmol of am-FeOOH)$^{-1}$ min^{-1}. The photoreduction process is somewhat slower in 0.1 M NaCl (initial rate $\simeq$ 40 nmol of Fe reduced (μmol of am-FeOOH)$^{-1}$ min^{-1}) with essentially complete reduction after 3 h. At pH 6.5 the initial rate of reduction is 1.4 nmol of Fe reduced (μmol of γ-FeOOH)$^{-1}$ min^{-1} with the Fe(II) concentration reaching a plateau at 0.18 μM (i.e., $\simeq$5% of total added Fe(III) reduced) after irradiation for $\simeq$2 h. (This rapid photodissolution of am-FeOOH complicates somewhat the results obtained with γ-FeOOH which has been shown to contain some amorphous material (*10*). However, the amorphous fraction does not exceed 10%; less than half of the fraction dissolved in 3 h in the

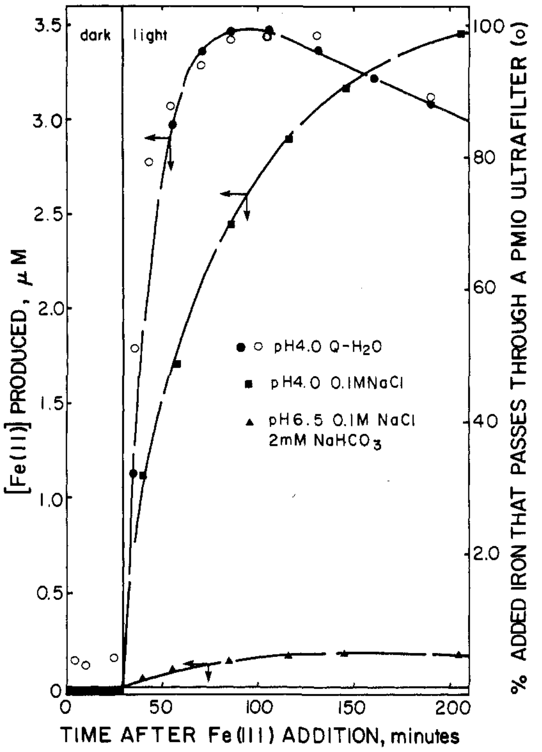

Figure 5. Production of Fe(II) as determined by phenanthroline colorimetry on irradiation of pH 4.0 solutions of Q-H_2O or 0.1 M NaCl and a pH 6.5 solution of 0.1 M NaCl-2 mM $NaHCO_3$ containing 3.5 μM Fe(III). The PM10 ultrafilterability of the iron in the pH 4.0 Q-H_2O study is also shown.

presence of fulvic acid (Figure 2). Since the observed dissolution rate is reasonably constant during that time, it is presumably not controlled by photodissolution of the amorphous fraction.)

These high initial rates and yields of Fe(II) are somewhat surprising in view of the frequent reports that the production of reduced iron on irradiation of solutions containing ferric hydroxy species is relatively low due to the efficiency of the back-reaction between the photoproducts Fe^{2+} and hydroxyl radicals (*4*). However, the rate of this back-reaction will be dependent on the Fe^{2+} and hydroxyl radical concentrations and may be relatively slow for low initial concentrations of Fe(III) (and hence low concentrations of the product, Fe^{2+}). Sharp increases in the yield of Fe(II) on decreasing the initial Fe(III) concentration have in fact been reported and satisfactorily modeled on the basis of the Fe^{2+} back-reaction rate (*28*).

A variety of possible mechanisms can be constructed to account for the observed photodissolution of amorphous iron oxide and production of ferrous iron. Previous studies of the photoredox chemistry of Fe(III) hydroxy species have been conducted at low pH (generally <2). The primary photoreaction in these homogeneous systems is considered to be (*28, 29*)

$$FeOH^{2+} \xrightarrow{h\nu} Fe^{2+} + \cdot OH \qquad (1)$$

More highly hydrolyzed species such as $Fe(OH)_2{}^+$ have been reported (*30*) to be photochemically less active than $FeOH^{2+}$ (or Fe^{3+}). A solution phase photoreaction similar to (1) may also be dominant in the heterogeneous systems considered here, with dissolution of the relatively soluble amorphous iron oxide colloids occurring in order to reestablish equilibrium as $FeOH^{2+}$ is consumed. However, dissolution of colloidal iron oxide induced through establishment of a disequilibrium condition is typically a relatively slow process and unlikely to yield the high rates of solubilization observed here (*31, 32*). A more likely alternative involves a hydroxylated ferric species at the colloid surface as primary chromophore. Even though the peak charge-transfer band of such surface hydroxy species occurs in the UV (*10*), near-UV irradiation should result in the direct release of some Fe^{2+} to solution:

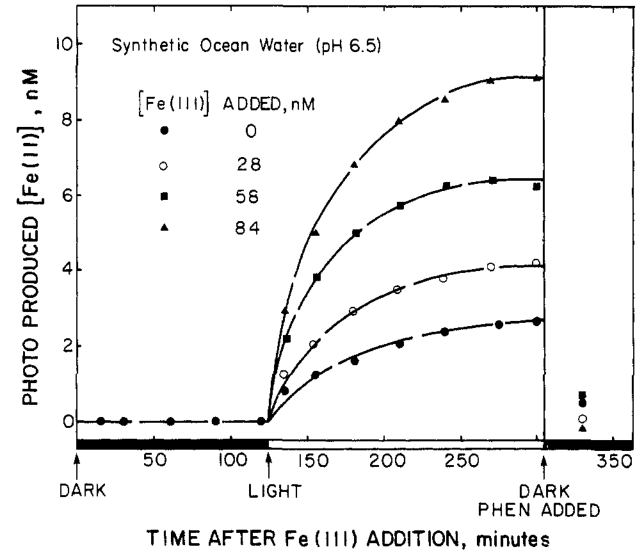

Figure 6. Production of coulometrically determined Fe(II) (i.e., Fe(II) that is electrochemically oxidizable at a working electrode potential of 0.45 V) on irradiation of pH 6.5 synthetic ocean water containing low concentrations of added ferric iron. The effect of addition of excess 1,10-phenanthroline is also shown. pH set by equilibration with 2.5% CO_2/air mixture and total radiation input = 30 μEinsteins mL^{-1} min^{-1}.

$$\equiv FeOH \xrightarrow{h\nu} Fe^{2+} + \text{oxidized products} \qquad (2)$$

In this case, as in the oxide–organic systems, the major factor governing dissolution under any given condition will be the primary chromophore concentration. If this mechanism is correct, then the particularly strong dependence of net iron oxide dissolution on pH (100% and 5% of added iron solubilized after 3 h at pH 4.0 and pH 6.5, respectively) is to be expected since the primary chromophore is most likely a monohydroxy ferric species—the concentration of which depends implicitly on pH. Alternatively, one could also speculate that most of the incident light is absorbed by the bulk of the FeOOH and that some of the resulting excited states migrate by an exciton-hopping mechanism to the colloid surface where Fe(III) is reduced and dissolved.

The increased photoreduction rate found on decreasing the chloride content has been observed previously (*28, 33*). While some debate exists concerning the mechanism of deactivation by chloride, the involvement of the $FeCl^{2+}$ species has been hypothesized. At the pH used by earlier workers, this species constituted a significant proportion of the total iron present. This is not the case under the conditions of this study (pH ≥4) where ferric hydroxy species dominate the Fe(III) chemistry. Another possible explanation involves the effect of ionic strength on coagulation kinetics. A decrease in ionic strength will lower the rate of coagulation of iron oxyhydroxide colloids with a resultant increase in colloidal surface area. Such a change should lead to an increase in the number of photoactive iron hydroxy surface sites and is thus consistent with mechanism 2. Note that the observed increase in photoreduction rate at pH 4.0 on changing from a 0.1 M NaCl solution to organic-free Q-H_2O also confirms that organic contamination of the salt is not responsible for the observed photoreduction phenomenon.

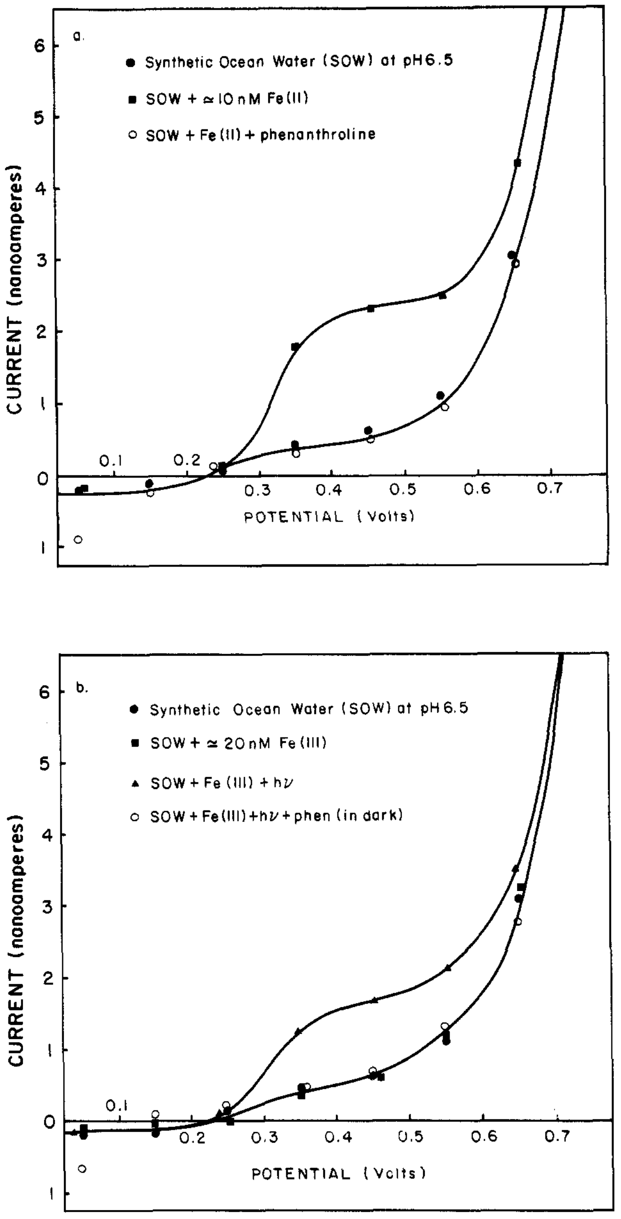

Figure 7. Steady-state voltage-current plots for pH 6.5 synthetic ocean water (a) before and after addition of ≃10 nM added Fe(II) and (b) before and after addition of ≃20 nM Fe(III) and subsequent irradiation. The effect of addition of excess 1,10-phenanthroline in both cases is also shown.

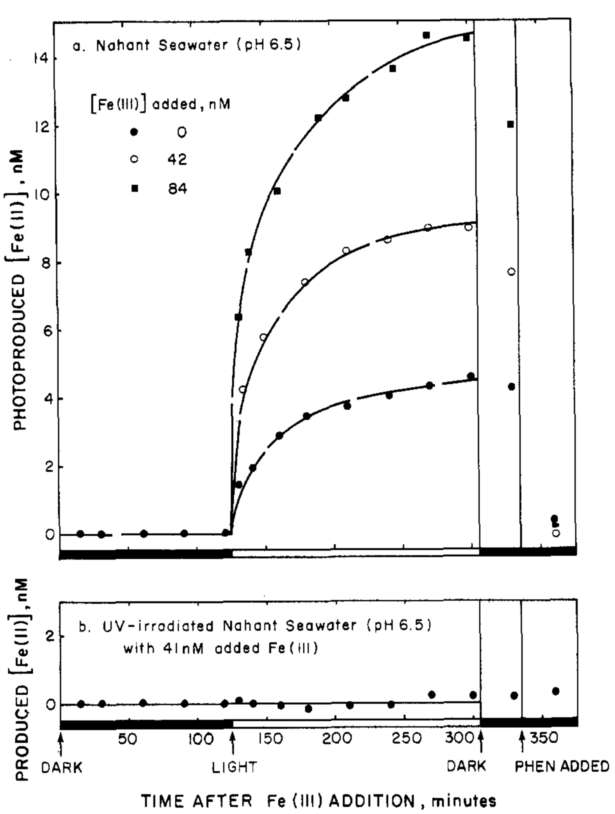

Figure 8. Production of coulometrically determined Fe(II) on irradiation of (a) pH 6.5, 0.2-μm filtered Nahant seawater containing added ferric iron and (b) UV-irradiated pH 6.5, 0.2-μm filtered Nahant seawater containing added ferric iron. The effects of subsequently ceasing irradiation and adding 1,10-phenanthroline are also shown.

Ferric iron reduction is also observed on irradiation of synthetic ocean water (SOW) buffered to pH 6.5 containing low concentrations of added Fe(III). As shown in Figure 6, a 2-h period of irradiation of pH 6.5 SOW containing 0, 28, 58 and 84 nM added Fe(III) results in the production of 2.7, 4.2, 6.4, and 9.1 nM Fe(II), respectively. This corresponds to a reduction of 6–7% of total added iron and is only slightly higher than the proportion of Fe(III) reduced in the high concentration, pH 6.5 studies discussed above (≃5%). The production of Fe(II) on irradiation of SOW containing no added iron presumably results from low-level iron contamination of the synthetic ocean water.

Production of Fe(II) on irradiation of SOW has been monitored by using the relatively nonspecific technique of controlled potential coulometry. That the oxidizable species produced is in fact Fe(II) is apparent on comparison of the "steady-state" voltage–current curves shown in Figure 7. The voltage–current response obtained on addition of Fe(II) to pH 6.5 SOW (Figure 7a) is essentially identical with the response observed after irradiation of SOW containing added Fe(III) (Figure 7b). The effect of 1,10-phenanthroline in masking these Fe(II) oxidation waves is also shown in Figure 7 (*17*). This masking technique has been used to add specificity in many of the coulometric studies performed here (as shown, for example, in Figure 6).

While a significant dissolution and concomitant reduction of colloidal amorphous iron oxide in organic-free synthetic ocean water is observed at pH 6.5, no such effects are apparent at the natural seawater pH of 8.2. This result is not particularly surprising in view of the dependence of initial dissolution rate on chromophore concentration. At pH 8.2, the concentration of the presumed surface-bound iron hydroxy chromophore is likely to be very low; thus, significant photodissolution is not to be expected. In addition, at pH 8.2, the rapid removal of photoproduced species from solution phase by oxidation to insoluble ferric oxyhydroxides will be a major effect limiting net photodissolution in these organic-free systems.

It appears then that in an organic-free system, iron hydroxy chromophores are present, with the less hydrolyzed species exhibiting high reactivity. Occurrence of photodissolution requires that these light absorbers be present at the particle surface; thus, factors affecting surface area (e.g., rate of coagulation, particle size, etc.) have a direct effect on dissolution rate. The chromophore specificity leads to a distinct pH dependence with the result that significant dissolution is only expected at acidic pH. Ferric photoreduction has been reported in other studies (*26, 27*) on very low pH systems (pH <2) where all iron is in soluble form; thus, it is apparent that the presence of solid species is not necessary for Fe(III) reduction to occur (a possibility originally suggested by Good and Purdon (*34, 35*)). However, it is possible that the charged colloid surface provides an electrostatic barrier to recom-

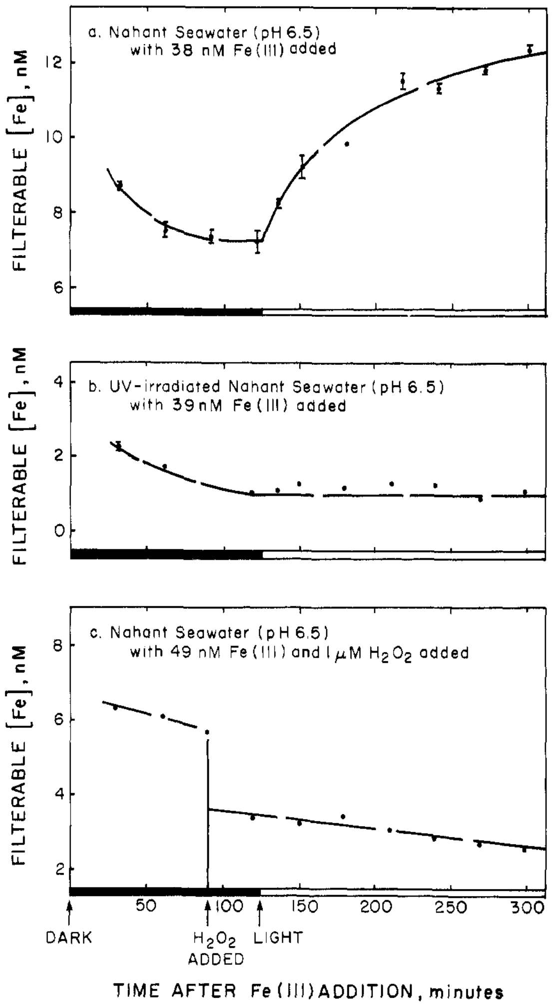

Figure 9. Change in PM10 ultrafilterability on irradiation of (a) pH 6.5, 0.2-μm filtered Nahant seawater containing added ferric iron, (b) UV-irradiated pH 6.5, 0.2-μm filtered Nahant seawater containing added ferric iron, and (c) pH 6.5, 0.2-μm filtered Nahant seawater containing added ferric iron and 1 μM H_2O_2.

bination of the photoproduced redox pair, thus enhancing reduction of the surface Fe(III) groups (*36*, *38*).

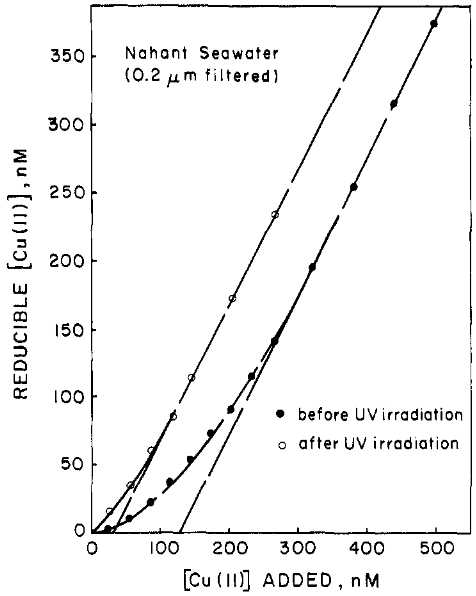

Figure 10. Results of Cu(II)/Cu(I) amperometric titrations of 0.2-μm filtered Nahant seawater before and after an 8-h period of UV irradiation.

Photodissolution of Amorphous Iron Oxide in Coastal Seawater. As shown in Figure 8a, irradiation of 0.2-μm filtered coastal seawater buffered to pH 6.5 with and without added Fe(III) results in the production of coulometrically determined ferrous iron (i.e., Fe(II) that is electrochemically oxidizable at a working electrode potential of 0.45 V). Additions of 0, 42, and 84 nM Fe(III) are seen to result in the production of 4.4, 9.0, and 14.5 nM Fe(II), respectively, after a 2-h period of irradiation. The produced Fe(II) exhibits a concentration-dependent decay on return to darkness and is completely masked by phenanthroline addition. As can be seen from the result of PM10 ultrafiltration studies in Figure 9a, the photoreduction of Fe(III) added to pH 6.5 Nahant seawater containing 38 nM added Fe(III) results in an increase in ultrafilterable iron of 5.0 ± 0.2 nM. This compares closely with a production of 4.7 ± 0.2 nM Fe(II) obtained on irradiating pH 6.5 Nahant seawater with 42 nM Fe(III) added (see Figure 8a). While significant colloidal dissolution and Fe(II) production is observed at pH 6.5, no such effects of irradiation are observed at the natural seawater pH of 8.2. Presumably, at this pH, the concentration of photoactive species is too low to allow observation of any effects of light. If solubilization/reduction processes are operating, the net changes in iron speciation occurs at concentrations below the detection limits of the electrochemical and size-separation/radiotracer techniques used here (i.e., ≃0.5 nM).

Interestingly, irradiation of filtered pH 6.5 Nahant seawater results in an initial reduction rate of 14 nmol of Fe(II) formed (μmol of am-FeOOH)$^{-1}$ min^{-1} and an average production after 2 h of 120 ± 10 nmol of Fe(II)/μmol of added Fe(III) while irradiation of pH 6.5 synthetic ocean water results in an initial reduction rate of only 3.2 nmol of Fe(II) formed (μmol of am-FeOOH)$^{-1}$ min^{-1} and an average production after 2 h of only 60 ± 10 nmol of Fe(II)/μmol of added Fe(III). The significantly higher degree of photoreduction observed for the coastal seawater compared to SOW may well be due to the presence of organic ligands which are capable of binding ferric iron to form photoactive species of greater lability than ferric hydroxy groups (possibly in a manner similar to that discussed above for freshwater fulvic acids). That relatively high concentrations of metal binding ligands are indeed present is shown by the results of Cu(II)/Cu(I) amperometric titrations (*18*) of the coastal seawater before and after long-term UV irradiation (see Figure 10). Cu(II) binding capacities of approximately 130 and 30 nM are obtained before and after UV irradiation, respectively; thus, an organic component capable of binding ≃100 nM of a divalent metal is apparently present. (The metal binding capacity remaining after UV irradiation may be attributed to non-UV destructible metal binding entities such as colloid surfaces.)

Surprisingly, the photoreduction and photodissolution effects previously observed for pH 6.5 Nahant seawater are completely eliminated on performing the same studies in pH 6.5, UV-irradiated Nahant seawater (see Figures 8b and 9b) rather than the expected result of partial reduction of the effects to the level of those observed in essentially organic-free synthetic ocean water. The most likely explanation for the dramatic effect of UV irradiation lies in the observed production of hydrogen peroxide. The results of peroxide analysis of two Nahant seawater samples before and after an 8-h period of UV irradiation are shown in Table I and indicate a peroxide production of approximately 1 μM on irradiation. Thus, after UV irradiation, peroxide will be in large excess of any photoproduced Fe(II) and will rapidly oxidize the ferrous iron (recall

Table I. Peroxide (H_2O_2 + Organic Peroxide) Concentrations As Determined by the Peroxidase–Scopoletin Method for Two Samples of 0.2-μm Filtered Coastal Seawater Obtained from the Same Location at Different Times before and after Long-Term (8 h) UV Irradiation

	peroxide concn, μM	
sample	before UV irradiation	after UV irradiation
1	0.56	1.46
2	0.47	1.56

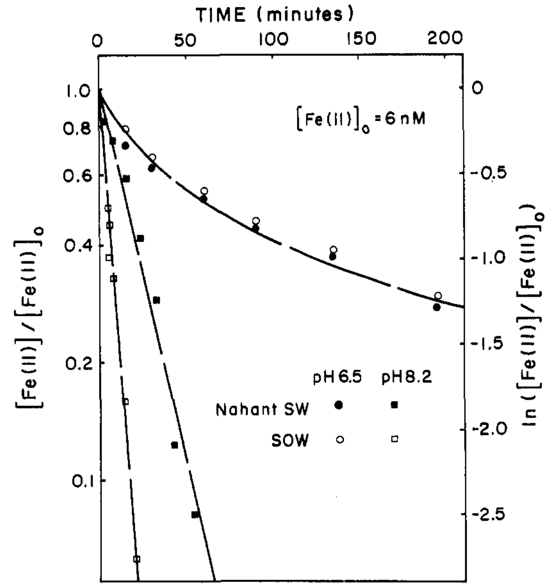

Figure 11. Controlled potential coulometric study of Fe(II) oxidation in synthetic ocean water (SOW) and coastal Nahant seawater at pH 6.5 and 8.2.

Figure 4). The effect of excess H_2O_2 in guaranteeing the removal of any Fe(II) is clearly seen from the results of a photodissolution study of pH 6.5 Nahant seawater containing added Fe(III) and 1 μM H_2O_2 (Figure 9c). Note that the results of the peroxidase–scopoletin test performed on the coastal seawater indicate that relatively high concentrations of peroxides are present in the natural seawater samples even before UV irradiation. Obviously, this "intrinsic" peroxide does not totally eliminate photoproduction of Fe(II), suggesting that it may not be available for participation in Fenton's reagent type oxidations.

As mentioned earlier, the concentration of photoproduced Fe(II) decreases on cessation of photolysis. Additional studies of this Fe(II) loss indicate that the process is not first order and occurs at approximately the same rate in both synthetic and natural seawater buffered to pH 6.5 (see Figure 11). The observed concentration change occurs much more rapidly than the expected rate of Fe(II) oxidation in a medium of high chloride content (*39*). The most probable removal mechanism involves adsorption of Fe(II) to the reaction vessel and working electrode and is possibly a major factor in determining the observed Fe(II) concentration in these low iron addition studies. Only at high pH where the Fe(II) oxidation rates are significantly greater than the rates of Fe(II) removal by adsorption do we observe first-order processes more typical of Fe(II) oxidation kinetics. Interestingly, the rate of Fe(II) removal in the coastal seawater ($\tau_{1/2} \simeq$ 16 min) is significantly lower than the rate observed in synthetic ocean water ($\tau_{1/2} \simeq$ 5 min) and, as found for Fe(II) oxidation studies in the presence of strong ferric chelators (*10*), may indicate retardation of the Fe(II) oxidation rate by naturally occurring organic complexing agents at this high (natural seawater) pH. It should be noted, however, that irradiation of natural seawater may produce hydrogen peroxide which is likely to remove any Fe(II) from solution very rapidly. Because of major cation competition, it is expected that complexation by naturally occurring organic matter would be too slow to prevent solid iron oxyhydroxide formation.

Table II. Initial Rates of Iron Oxide Photodissolution under a Variety of Conditions[a]

	initial rate of iron oxide dissolution[b] (nmol of Fe solubilized (μmol of FeOOH)$^{-1}$ min^{-1})		
conditions	pH 4.0	pH 6.5	pH 8.2
(a) no organic			
γ-FeOOH in 0.1 M NaCl	0.26	<0.05	
am-FeOOH in 0.1 M NaCl	40	1.4	<0.05
am-FeOOH in SOW		3.2	<0.05
(b) organic present			
γ-FeOOH in 0.1 M NaCl + 10 mg/L fulvic acid	1.10	0.28[c]	
am-FeOOH in coastal seawater		14	<0.05

[a] Total radiation input of 30 μEinsteins mL^{-1} min^{-1} used in all cases. [b] Estimated detection limit for rate determination by both colorimetric and coulometric procedures. [c] Average of values for two fulvic acids.

Photoproduction of H_2O_2 and resultant oxidation of photoproduced Fe(II) to the insoluble ferric oxyhydroxide form may well account for the marked decrease observed on continued photolysis in the rate of dissolution of am-FeOOH added to pH 6.5 Nahant seawater. As noted above, the initial rate of am-FeOOH photodissolution is very high in this CO_2-buffered coastal seawater and is 4–5 times that observed in pH 6.5 SOW. Despite this high initial rate, the final steady-state concentration of Fe(II) in the Nahant seawater is only double that obtained in SOW and may be due to H_2O_2-induced back-reactions removing Fe(II) from solution on continued photolysis in Nahant seawater but not in organic-free SOW.

Summary

A compilation of initial rates of iron oxide photodissolution obtained under various conditions is given in Table II and provides a useful means of reviewing the essential aspects of this study. In the absence of organic agents, iron oxides are solubilized to varying degrees through photodissociation of ferric hydroxy groups (particularly the less hydrolyzed species) at the colloid surface. The rate of dissolution is dependent principally on the chromophore concentration and is thus influenced directly by factors such as pH and particle size. For example, we observe a high rate of dissolution for the very small amorphous iron oxide colloids at low pH (pH 4.0, 0.1 M NaCl) and a marked decrease in dissolution rate as the pH is increased and the surface ferric sites become more hydrolyzed (and less photoactive). The rate of dissolution of larger, more insoluble lepidocrocite particles under similar conditions is considerably less presumably because of the lower surface area with the result that, for a given oxide concentration, fewer photoactive surface sites are present. It is not surprising that, given the pH dependence of chromophore concentration, no detectable dissolution is observed at high pH. Rapid oxygenation reactions removing photoproduced Fe(II) from solution are, no doubt, also of significance in limiting net dissolution at high pH.

The effect of naturally occurring organic materials is to significantly increase the initial rate of dissolution in all observable cases. Thus, at pH 4.0, addition of excess fulvic acid to a γ-FeOOH suspension enhances the dissolution rate by a factor of 4. Similarly, photodissolution studies performed on amorphous iron oxide in coastal seawater buffered to pH 6.5 yield a dissolution rate of 14 nmol of Fe solubilized (μmol of am-FeOOH)$^{-1}$ min^{-1}, a rate 4–5 times that observed in essentially organic-free synthetic ocean water. Freshwater fulvic acids induce a photodissolution process similar to that previously observed with citrate. It is likely that the governing mechanisms are similar in both cases though the possibility of direct excitation of the fulvic acid molecule by near-UV radiation (which is unlikely for citrate) with subsequent reduction of Fe(III) cannot be ignored. A major difference in the case of naturally occurring organic acids involves the formation of the powerful oxidant hydrogen peroxide. In freshwater systems, the generation of this agent will perturb the solution speciation of iron significantly but, unless the rate of Fe(III) complexation by the organic material present is particularly slow, should not markedly affect the net dissolution of iron oxides (at least in the short term). This is to be compared with the effect in seawater, where major cation competition for organic ligands may retard the complexation of ferric iron. Under these conditions, insoluble iron oxides are likely to form instead of soluble Fe(III)–organic complexes.

Despite the apparent enhancement in photoactivity of iron groups in the presence of organic agents at pH 4.0 and pH 6.5, no light-induced changes in iron speciation are observed at pH 8.2 (in freshwater or marine systems). Thus, significant effects of light on Fe chemistry can only be expected in low pH waters or microenvironments, even though the pH dependency of chromophore concentration is not likely to be as marked for iron–organic groups as it is for ferric hydroxy entities.

Registry No. Iron oxide, 1332-37-2.

Literature Cited

(1) Zafiriou, O. C. In "Chemical Oceanography"; Riley, J. P.; Chester, R., Eds.; Academic Press: London, 1983; 2nd ed., Vol.8 Chapter 48, pp 339–379.
(2) Zepp, R. G. In "Dynamics, Exposure and Hazard Assessment of Toxic Chemicals"; Haque, R., Ed.; Ann Arbor Science: Ann Arbor, MI, 1980.
(3) Conrad, R.; Seiler, W.; Bunse, G.; Giehl, H. *J. Geophys. Res.* **1982**, *87*, 8839–8852.
(4) Balzani, V.; Carassiti, V. "Photochemistry of Coordination Compounds"; Academic Press: New York, 1970.
(5) McMahon, J. W. *Limnol. Oceanogr.* **1969**, *14*, 357–367.
(6) Miles, C. J.; Brezonik, P. L. *Environ. Sci. Technol.* **1981**, *15*, 1089–1095.
(7) Francko, D. A.; Heath, R. T. *Limnol. Oceanogr.* **1982**, *27*, 564–569.
(8) Collienne, R. J. *Limnol. Oceanogr.* **1983**, *28*, 83–100.
(9) Anderson, M. A.; Morel, F. M. M. *Limnol. Oceanogr.* **1982**, *27*, 789–813.
(10) Waite, T. D.; Morel, F. M. M. *J. Colloid Interface Sci.*, in press.
(11) Waite, T. D.; Morel, F. M. M. *Anal. Chim. Acta*, in press.
(12) Walling, C. *Acc. Chem. Res.* **1975**, *8*, 125–131.
(13) VanBaalen, C.; Marler, J. E. *Nature (London)* **1966**, *211*, 951.
(14) Cooper, W. J.; Zika, R. G. *Science (Washington, D.C.)* **1983**, *220*, 711–712.
(15) Draper, W. M.; Crosby, D. G. *Arch. Environ. Contam. Toxicol.* **1983**, *12*, 121–126.
(16) Zika, R. G.; Zelmer, P.; Petasne, R., 1984, unpublished results.
(17) Waite, T. D.; Morel, F. M. M. *Anal. Chem.* **1984**, *56*, 787–792.
(18) Waite, T. D.; Morel, F. M. M. *Anal. Chem.* **1983**, *55*, 1268–1274.
(19) Thurman, E. M.; Malcolm, R. L. In "Aquatic and Terrestial Humic Materials"; Christman, R. F.; Gjessing, E. G., Eds.; Ann Arbor Science: Ann Arbor, MI, 1983; Chapter 1, pp 1–23.
(20) Thurman, E. M.; Malcolm, R. L. *Environ. Sci. Technol.* **1981**, *15*, 463–466.
(21) Morel, F. M. M.; Rueter, J. G.; Anderson, D. M.; Guillard, R. L. L. *J. Phycol.* **1979**, *15*, 135–141.
(22) Parker, C. A. "Photoluminescence of Solutions with Application to Photochemistry and Analytical Chemistry"; Elsevier: Amsterdam, 1968; pp 478–481.
(23) Watanabe, T.; Takizawa, T.; Honda, K. *J. Phys. Chem.* **1977**, *81*, 1845–1851.
(24) Zika, R. G. In "Marine Organic Chemistry"; Duursma, E. G.; Dawson, R., Eds.; Elsevier: Amsterdam, 1981; Chapter 10, pp 299–326.
(25) Sawyer, D. T.; Valentine, J. S. *Acc. Chem. Res.* **1981**, *14*, 393–400.
(26) Baxter, R. M.; Carey, J. H. *Nature (London)* **1983**, *306*, 575–576.
(27) Bonneau, R.; Pottier, R.; Bagno, O.; Joussot-Dubien, J. *Photochem. Photobiol.* **1975**, *21*, 159–163.
(28) David, F.; David, P. G. *J. Phys. Chem.* **1976**, *80*, 579–583.
(29) Buxton, G. V.; Wilford, S. P.; Williams, R. J. *J. Chem. Soc.* **1962**, 4957–4962.
(30) Mulay, L. N.; Selwood, P. W. *J. Am. Chem. Soc.* **1955**, *77*, 2693.
(31) Valverde, N.; Wagner, C. *Ber. Bunsenges. Phys. Chem.* **1976**, *80*, 330–333.
(32) Valverde, N. *Ber. Bunsenges. Phys. Chem.* **1976**, *80*, 333–340.
(33) Langford, C. H.; Carey, J. H. *Can. J. Chem.* **1975**, *53*, 2430–2435.
(34) Good, W.; Purdon, W. A. B. *Chem. Ind. (London)* **1955**, 144–145.
(35) Good, W.; Purdon, W. A. B. *Chem. Ind. (London)* **1955**, 1594–1595.
(36) Gratzel, M. *Acc. Chem. Res.* **1981**, *14*, 376–384.
(37) Matsuo, T. *Pure Appl. Chem.* **1982**, *54*, 1693–1703.
(38) Calvin, M. *Photochem. Photobiol.* **1983**, *37*, 349–360.
(39) Sung, W.; Morgan, J. J. *Environ. Sci. Technol.* **1980**, *14*, 561–568.

Received for review January 3, 1984. Accepted June 11, 1984. This work was supported in part by NSF Grant OCE-8119103 and NOAA Grant NS79AA-D-00077.